Journal Pre-proof

Treatment of Landfill Leachate Using Magnetically Attracted Zero-valent Iron Powder Electrode in an Electric Field

Dongni Sun (Writing - original draft) (Data curation) (Formal analysis)<ce:contributor-role>Validation; Investigation) (Software) (Methodology), Xiaoting Hong (Writing - original draft) (Conceptualization) (Methodology) (Project administration) (Funding acquisition) (Writing - review and editing) (Supervision) (Resources) (Methodology), Zhonghua Cui (Data curation) (Software), Yingying Du (Investigation) (Software), K.S. Hui (Writing - review and editing), Enhao Zhu (Investigation), Keming Wu (Formal analysis), K.N. Hui (Writing - review and editing)

This is a PDF file of an article that has undergone enhancements after acceptance, such as the addition of a cover page and metadata, and formatting for readability, but it is not yet the definitive version of record. This version will undergo additional copyediting, typesetting and review before it is published in its final form, but we are providing this version to give early visibility of the article. Please note that, during the production process, errors may be discovered which could affect the content, and all legal disclaimers that apply to the journal pertain.

Treatment of Landfill Leachate Using Magnetically Attracted Zero-valent Iron Powder Electrode in an Electric Field

Dongni Sun[a,b], Xiaoting Hong[a,*], Zhonghua Cui[c], Yingying Du[a], K.S. Hui[d], Enhao Zhu[a], Keming Wu[b], K. N. Hui[e]

[a] Department of Chemistry, Zhejiang Sci-tech University, Hangzhou 310018, P.R. China

[b] State Environment Protection Key Laboratory of Mineral Metallurgical Resources Utilization and Pollution Control, Wuhan University of Science and Technology, Wuhan 430081, P.R. China

[c] School of Environment and Natural Resources, Zhejiang University of Science and Technology, Hangzhou 310023, P.R. China
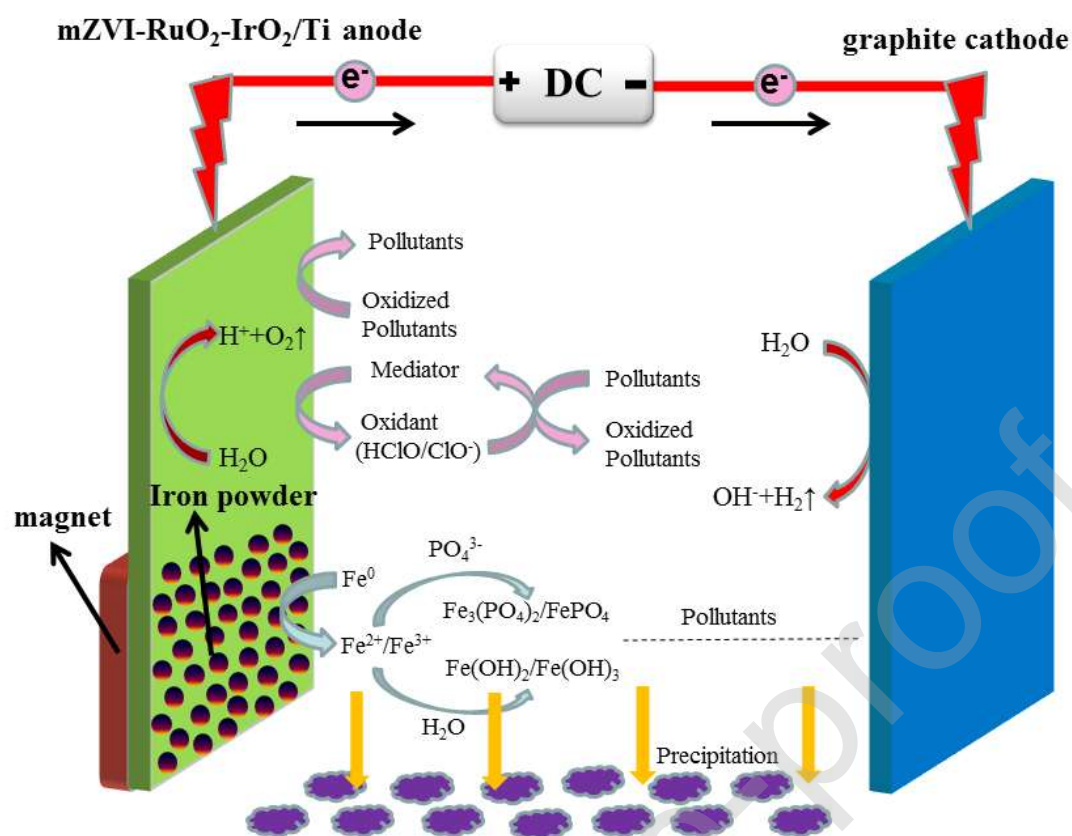
[d] School of Engineering, Faculty of Science, University of East Anglia, Norwich, NR4 7TJ, United Kingdom

[e] Institute of Applied Physics and Materials Engineering, University of Macau, Avenida da Universidade, Taipa, Macau, China

Corresponding author. Tel.: +86 (0571) 86843228, Fax +86 (0571) 86843228.

E-mail address: hanren.xiaoting@gmail.com (X.T. Hong).

Graphical abstract

Highlights

► RuO$_2$-IrO$_2$/Ti plate combined with iron powder acting as an anode of electrochemical unit.

► Iron powders were immobilized at the surface of the RuO$_2$-IrO$_2$/Ti plate by a magnet.

► The mZVI-RuO$_2$-IrO$_2$/Ti anode showed high removal efficiency of N, P, TOC and metals.

► Elemental composition and the type of the reaction product were characterized by SEM-EDS, XRD and XPS.

Abstract: This study combined electro-oxidation (EO) and electrocoagulation (EC) process (EO/EC) to treat landfill leachate by using RuO$_2$-IrO$_2$/Ti plate and microscale zero-valent iron powder composite anode. EO was achieved by direct oxidation and indirect oxidation on RuO$_2$-IrO$_2$/Ti plate, whereas EC was achieved using iron powder

to lose electrons and produce coagulants in situ. The influences of variables including type of anode material, applied voltage, zero-valent iron dosage, interelectrode gap, and reaction temperature on EO/EC were evaluated. Results showed that at an applied voltage of 10 V, zero-valent iron dosage of 0.2 g, interelectrode gap of 1 cm, and non-temperature-controlled mode, the removal efficiencies were 72.5% for total organic carbon (TOC), 98.5% for ammonia, and 98.6% for total phosphorus (TP). Some heavy metals and hardness were also removed. Further analysis indicated that the removal of TOC, ammonia, and TP followed pseudo-first order, pseudo-zero order, and pseudo-second order kinetic models, respectively. Other characteristics were examined by scanning electron microscopy–energy dispersive spectrometry, X-ray diffraction, and X-ray photoelectron spectroscopy. Overall, our results showed that EO/EC can be used to efficiently remove organic matter, ammonia, TP, and heavy metals from landfill leachate.

Key words: landfill leachate; electro-oxidation; electrocoagulation; zero-valent iron

1. Introduction

In recent years, the increasing population, acceleration of industrialization, and continuous development of the economy have led to the rapid increase in municipal and industrial solid-waste production; the sanitary landfill method is a widely accepted and used method for waste treatment due to its economic advantages [1]. Leachates result

3

from rain passing through a landfill site and from the liquid generated by the breakdown of the waste within the landfill [2]. Landfill leachate contains a large number of compounds, such as organic and inorganic compounds and heavy metals. Release of these toxic and harmful substances into the natural environment may cause pollution of groundwater, surface water, and soil, posing a threat to human health and nature [3, 4].

Landfill leachate is generally known as high-strength wastewater because its composition is extremely complex and varies greatly, making it extremely difficult to deal with [5]. Some studies have reported that leachate can be treated by biological and physicochemical methods [6]. Biological methods include treatment of landfill leachate by aerobic or anaerobic processes [7]. However, when dealing with low-biodegradability landfill leachate, biological treatment may not achieve good results due to the stubborn nature of organic carbon in leachates [8]. Therefore, physicochemical treatment of landfill leachate has received more attention. The method for treating stabilized landfill leachate includes coagulation-flocculation [9], Fenton processes [10], chemical precipitation [11], nanofiltration, and reverse osmosis [12, 13]. Over the past decade, advanced electrochemical technologies for the treatment of landfill leachates, such as electro-oxidation (EO), electrocoagulation (EC), and electro-Fenton, have received increasing attention due to the increased efficiencies that can be achieved using easy to operate and control, as well as compact bipolar electrochemical reactors [14, 15].

EO, as one of the advanced oxidation processes, can significantly reduce the

4

concentration of organic pollutants and ammonia in landfill leachate by direct oxidation and indirect oxidation [16]. Contaminants, such as organic compounds and ammonia, can be oxidized and removed by direct electron transfer on the anode surface [16]. Contaminants can also be degraded by indirect oxidation, in which a mediator is electrochemically generated to carry out the oxidation where active chlorine is the primary indirect oxidant used in wastewater treatment [15, 17]. Anode materials are receiving extensive attention as an important factor in the process of EO [18]. Boron-doped diamond anode is used to treat landfill leachate with low BOD_5/ COD ratio; chemical oxygen demand (COD), total nitrogen (TN), and color were all reduced [19]. Titanium coated with metal oxide (PbO_2, SnO_2), which was used as the anode, can reduce the COD and remove almost all of the ammonia from the landfill leachate [20]. Mixed metal oxides (RuO_2-IrO_2/Ti) have been investigated for the effective degradation of tetracycline by electrochemical anodic oxidation process [21]. Moraes et al. investigated the effect of current efficiency on TOC, COD, ammonia, and color removal when RuO_2-IrO_2/Ti is used as anode for the treatment of landfill leachate [22].

EC requires simple equipment that is easy to operate and avoids the use of chemicals. It is a technology that produces small amounts of sludge, and flocs formed by EC can be separated faster by filtration; hence, it is widely used for wastewater treatment [23, 24]. EC involves the production of coagulants by electrolysis of metal ions from metal anodes, and the most common anode materials are iron and aluminum [25]. Sun et al. investigated the treatment of nanofiltration concentrate from landfill leachate by EC

with aluminum anode, and the treatment efficiencies for COD, color, and phosphorus were determined as 45%, 60%, and 91.8%, respectively [26]. Bouhezila et al. used iron as an anode to remove COD, TN, color, turbidity, and bacteria from landfill leachate by EC process [27]. Ilhan et al. evaluated the effects of various experimental parameters, including current density, pH, treatment cost, and operating time on the landfill leachate treatment by EC process using iron and aluminum anodes [28].

In recent years, to improve the efficiency of pollutant degradation, a combination of different electrochemical processes in the treatment of wastewater has been investigated. Mahvi et al. designed an EC/EO–electroflotation reactor for simultaneous removal of ammonia and phosphate from wastewater effluent [29]. Esfandyari et al. investigated aluminum, stainless steel, and RuO_2/Ti plates as electrodes for the treatment of olive mill wastewater by peroxi-EC/EO-EF process [30]. Li et al. combined the EO and EC processes using RuO_2-IrO_2/Ti as the anode and aluminum as the cathode to treat mature landfill leachate; 83.7% COD and 100% ammonia removal were achieved under optimum conditions [31]. Ding et al. investigated the EO/EC/electroreduction process for tertiary landfill leachate treatment, and such process removed 50%−60% organic matter and 100% ammonia under optimum conditions [32]. Based on these previous studies, organic matter and ammonia can be removed through EO, whereas organic matter and phosphorus can be removed through EC. However, in previous studies, achieving simultaneous EO and EC by using a single anode was difficult.

In this work, we combined EO and EC processes (EO/EC) for landfill leachate treatment by designing a RuO_2-IrO_2/Ti plate and microscale zero-valent iron powder composite electrode (mZVI-RuO_2-IrO_2/Ti). This EO/EC process, which used mZVI-RuO_2-IrO_2/Ti as anode and graphite plate as cathode, was developed and applied for the treatment of landfill leachate. The aim of this work was to evaluate the performance of this EO/EC process for the removal of organic, phosphorus, and nitrogen contaminants. Performance evaluation included the effects of several parameters, such as type of anode materials, applied voltage, zero-valent iron dosage, interelectrode gap, and reaction temperature. The kinetics of pollutant degradation has also been studied. The characteristics of the precipitates were investigated by scanning electron microscopy-energy dispersive spectrometer (SEM-EDS), X-ray diffraction (XRD), and X-ray photoelectron spectroscopy (XPS).

2. Materials and methods

2.1 Characteristics of landfill leachate

The leachate used in this study was obtained from an aging landfill leachate sampled from a municipal landfill in Zhejiang Province, China. Samples were collected in July 2018 and stored in a refrigerator at 4 °C until use. The concentrations of organic compounds and ammonia in the sample are extremely high. Electrolytes were not required when performing electrochemical treatment due to the good conductivity of the samples. The characteristics of the landfill leachate are listed in Table 1.

Table 1 Characteristics of the leachate samples

Parameters	Range	Average
TOC (mg·L^{-1})	3043.5-3185.5	3114.5
COD (mg·L^{-1})	1735-1865	1800
NH$_4^+$-N (mg·L^{-1})	1676.7-1751.1	1713.9
Cl$^-$ (mg·L^{-1})	2399-2424	2411.5
pH	8.34-8.65	8.5
Conductivity (mS·cm^{-1})	17.32-18.21	17.77
Total phosphorus (mg·L^{-1})	18.25-19.56	18.91
Calcium (mg·L^{-1})	56.3-60.7	58.5
Magnesium (mg·L^{-1})	66.4-71.1	68.75

2.2 Experimental setup and operation

All batch mode experiments were conducted in an open glass reactor (5 cm × 5 cm × 10 cm) at room temperature. 200 mL of the leachate was transferred into the reactor. The mZVI-RuO$_2$-IrO$_2$/Ti anode consists of a RuO$_2$-IrO$_2$/Ti plate (2.5 cm × 10 cm) and microscale zero-valent iron powder. ZVI powder (0.1 to 0.4 g) was applied evenly to an 8 cm^2 (2 cm × 4 cm) area at the bottom of the RuO$_2$-IrO$_2$/Ti plate. The mZVI powder was fixed on the surface of the RuO$_2$-IrO$_2$/Ti plate through a magnet (2 cm × 4 cm) outside the glass reactor as a mZVI-RuO$_2$-IrO$_2$/Ti composite anode. The mZVI-graphite and nZVI-RuO$_2$-IrO$_2$/Ti composite anodes were prepared by replacing the RuO$_2$-IrO$_2$/Ti plate with graphite sheets and replacing the mZVI powder with nanoscale zero-valent iron (nZVI) powder. The area of the RuO$_2$-IrO$_2$/Ti plate immersed in the solution was 15 cm^2. The electric power for this process was obtained from a dual-channel direct current power supply (Lodestar LPS325D, China). The anode and cathode were placed in parallel, and the interelectrode gap maintained a constant distance according to the

experimental design. The experimental setup is shown in Fig. S1.

Factors influencing the removal of organic compound, ammonia, and total phosphorus (TP) in the EO/EC process were investigated. Such factors included the type of anode materials (mZVI-RuO$_2$-IrO$_2$/Ti, nZVI-RuO$_2$-IrO$_2$/Ti, RuO$_2$-IrO$_2$/Ti, and mZVI-graphite), applied voltage (4, 6, 8, and 10 V), zero-valent iron dosage (0.1, 0.2, 0.3, and 0.4 g), interelectrode gap (0.5, 1, 1.5, and 2 cm), and reaction temperature (room temperature, 35, 45, and 55 °C). Each experiment was operated in batch mode and lasted for 6 h. Samples were taken from the EO/EC reactor for subsequent analysis at designated times during the experiment.

2.3 Analytical methods

Ammonia (NH$_4^+$-N) was determined with continuous flowing analyzer (Seal AA3, Germany). TP concentration was determined using a continuous flowing analyzer (Seal AA3, Germany) after high-temperature and high-pressure digestion by using a high-pressure steam sterilizer (STIK MJ-54A, America). TOC was determined with a Total Organic Carbon Analyzer (Shimadzu TOC-L, Japan). COD was determined by a fast digestion-spectrophotometric method using a HACH COD Analyzer (Hach DRB 200 and DR 1010, America). The type and content of heavy metals were determined by inductively coupled plasma optical emission spectrometry. The conductivity and pH of the solution were determined with a conductivity meter (Rex Chemical Corp., Shanghai) and pH meter (Mettler-Toledo, Switzerland). The surface morphologies, atomic composition, and distribution of the precipitate were obtained with a scanning electron

9

microscope-energy dispersive spectrometer (Phenom ProX, Phenom-World, Netherlands). The crystal structure of the precipitate after EO/EC was characterized using an X-ray diffractometer with Cu Kα radiation, where the 2θ scanning range is from 10° to 80° (PANalytical X'Pert PRO, Netherlands). XPS measurements were carried out with a Thermo Fisher Scientific ESCALAB 250Xi XPS spectrometer (Thermo Fisher Scientific ESCALAB 250Xi XPS spectrometer, America) using Al Kα radiation with photon energy of 1486.6 eV as the radiation source.

The removal efficiencies were calculated based on the initial and final concentrations and can be expressed as:

$$\eta = \frac{C_0 - C_t}{C_0} \times 100\% \tag{1}$$

where η is the NH_4^+-N, TP, or TOC removal efficiencies; C_0 is the initial concentration ($mg \cdot L^{-1}$) of NH_4^+-N, TP, or TOC; and C_t is the final concentration ($mg \cdot L^{-1}$) of NH_4^+-N, TP, or TOC.

3. Results and discussion

3.1 Influence factors of EO/EC process

3.1.1 Type of anode materials

Fig. 1 shows the removal of TOC, ammonia, TP, and COD during EO/EC process with different anodes. The TOC removal efficiencies using RuO_2-IrO_2/Ti, nZVI-RuO_2-IrO_2/Ti, and mZVI-RuO_2-IrO_2/Ti anodes can reach 64.4%, 71.4%, and 72.1%, respectively (Fig. 1a). By comparing the RuO_2-IrO_2/Ti and mZVI-graphite anodes, we

can conclude that the removal of TOC was primarily due to the EO process rather than the EC process. However, the TOC removal efficiency using mZVI-RuO$_2$-IrO$_2$/Ti anode was not considerably higher than that using RuO$_2$-IrO$_2$/Ti anode. This finding indicates the removal of organics by coagulation in addition to oxidation. We also studied the effect of ZVI powder particle size on the EO/EC process and concluded that the particle size of ZVI has little effect on the removal of TOC. COD removal exhibited a similar trend to that of TOC removal (Fig. 1d).

As seen in Fig. 1b, the mZVI-RuO$_2$-IrO$_2$/Ti, nZVI-RuO$_2$-IrO$_2$/Ti, and RuO$_2$-IrO$_2$/Ti anodes were considerably better than the mZVI-graphite anode for ammonia removal. Ammonia was primarily oxidized by anodic oxidation to produce intermediate oxidation products (Cl$_2$, HClO, and ClO$^-$). The main reactions were as follows [33]:

Anode:

$$2Cl^-\rightarrow Cl_2+2e^- \tag{2}$$

Aqueous phase:

$$Cl_2+H_2O\leftrightarrow HClO+H^++Cl^- \tag{3}$$

$$HClO\leftrightarrow H^++ClO^- \tag{4}$$

$$3HClO+2NH_4^+\rightarrow N_2+3H_2O+5H^++3Cl^- \tag{5}$$

Cathode:

$$2H_2O+2e^-\rightarrow H_2+2OH^- \tag{6}$$

Figure S3 shows a slight accumulation of nitrate during the EO/EC process. After 6 hours of electrolysis, the nitrate nitrogen in the leachate increased from an initial value of 7.6 mg·L^{-1} to 75.8 mg·L^{-1}. This also indicated that the ammonia in the leachate was
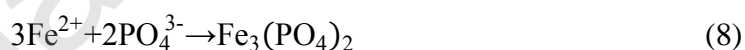
not completely oxidized to nitrogen, and a very small amount was oxidized to nitrate nitrogen. The mZVI-graphite anode removes only 29.3% of ammonia, which can be explained by the fact that the RuO_2-IrO_2/Ti anode has a higher oxygen evolution potential than the graphite electrode, and the surface of the graphite electrode was prone to oxygen evolution side reaction, resulting in less intermediate oxidation product [34]. The use of nZVI-RuO_2-IrO_2/Ti resulted in slightly lower ammonia removal efficiency than that by using mZVI-RuO_2-IrO_2/Ti and RuO_2-IrO_2/Ti anodes. This finding confirms the superiority of micron zero-valent iron composite anode in EO/EC process.

However, the mZVI-graphite anode, which performs poorly in removing organics and ammonia, demonstrated excellent performance for TP removal (Fig. 1c). TP was primarily removed by EC process, and the main reactions were as follows [35]:
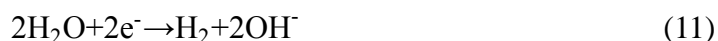
Anode:

$$Fe \rightarrow Fe^{2+} + 2e^- \tag{7}$$

Aqueous phase:

$$3Fe^{2+} + 2PO_4^{3-} \rightarrow Fe_3(PO_4)_2 \tag{8}$$

$$4Fe^{2+} + O_2 + 2H_2O \rightarrow 4Fe^{3+} + 4OH^- \tag{9}$$

$$Fe^{3+} + PO_4^{3-} \rightarrow FePO_4 \tag{10}$$

Cathode:

$$2H_2O + 2e^- \rightarrow H_2 + 2OH^- \tag{11}$$

ZVI powder acted as a sacrificial anode to dissolve Fe^{2+}/Fe^{3+} and formed iron-phosphorus compounds with phosphate in the leachate, and organic phosphorus was removed through coagulation by the generated $Fe(OH)_2$ or $Fe(OH)_3$. When the RuO_2-

IrO$_2$/Ti plate was used as the anode, 74.3% of the TP was still removed, although only EO process occurred. It can be considered that during electrolysis suspended solids in the leachate agglomerate into flocs which will absorb phosphorus. Moreover, a large amount of bubbles was generated during electrolysis, and many suspended solids were removed by air flotation. The TP concentration in the bubble was 7.75 mg·L^{-1}. Table 2 shows that the EO/EC system using mZVI-RuO$_2$-IrO$_2$/Ti as anode has a good effect on the removal of heavy metals and hardness. The content of heavy metals in landfill leachate was low, whereas the calcium and magnesium contents were relatively high. The heavy metal ions in the landfill leachate were removed through several processes (metal deposition on the cathode, precipitation, and co-precipitation of metals), and the most important is the iron hydroxide with high adsorption capacity produced by anodic dissolution, metal ions were removed together with the hydroxides as sludge [36]. In addition, some of the metal cations may also be removed by direct formation of hydroxide precipitates with OH$^-$ in the leachate [37]. This finding confirmed the feasibility of using mZVI-RuO$_2$-IrO$_2$/Ti anode for simultaneous removal of organics, ammonia, TP, and heavy metals from landfill leachate by combining EO and EC.
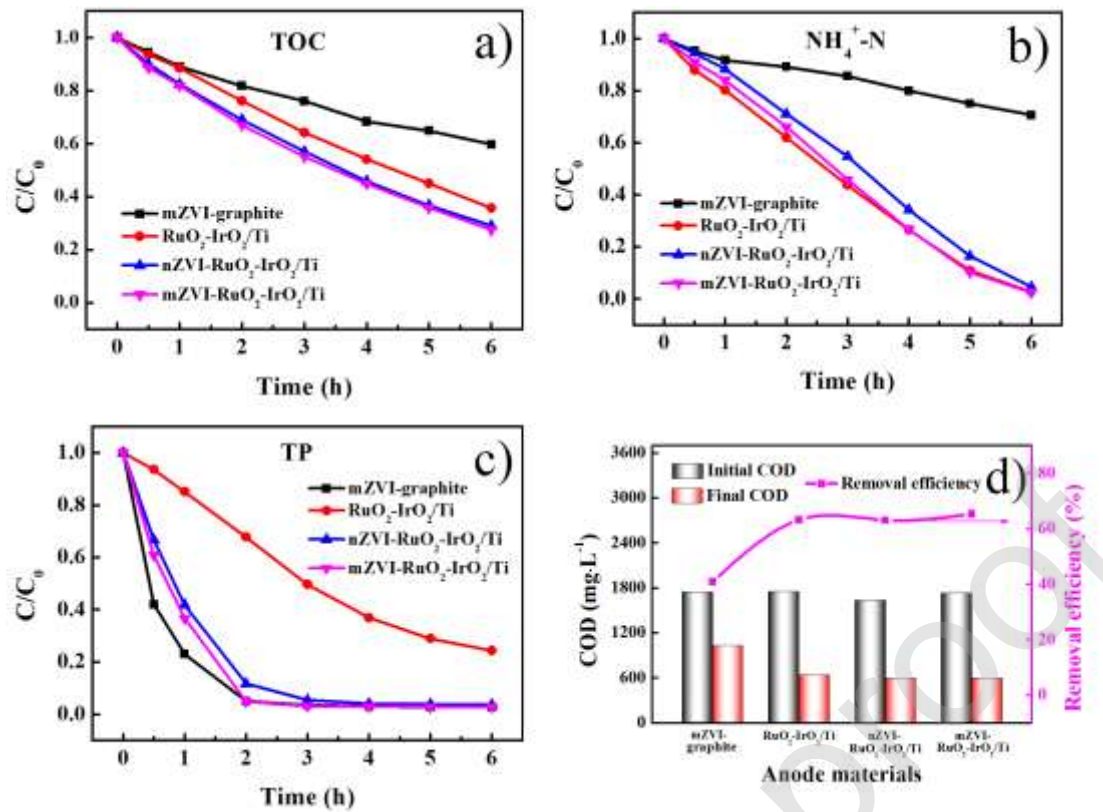
Fig. 1. a) TOC, b) NH_4^+-N, c) TP, and d) COD removal using different types of anode

materials.

Table 2 Metal removal by EO/EC process using mZVI-RuO$_2$-IrO$_2$/Ti anode

Species	Initial concentration (mg·L^{-1})	Final concentration (mg·L^{-1})	Removal efficiencies (%)
Ba	0.267	0.002	99.070
Ca	62.062	7.707	87.582
Co	0.053	0.004	91.765
Cr	0.226	0.021	90.659
Cu	0.110	0.016	85.876
Fe	3.722	0.915	75.429
Mg	71.734	1.387	98.067
Mn	0.560	Not detected	100.000
Ni	0.164	0.024	85.606
Zn	0.546	0.255	53.348

3.1.2 Applied voltage

The operational mode of the electrochemical treatment of wastewater involves

14

constant current or constant voltage. Experiments were performed at a constant voltage

mode in this study; given that the actual surface area of the composite electrode was

difficult to calculate, accurate current density was difficult to obtain. Although the

RuO_2-IrO_2/Ti plate has an area of 8 cm^2 for the uniform coating of iron powder, the ZVI

powder agglomerated in a small range and erected on the surface of the RuO_2-IrO_2/Ti

plate with a needle shape in a magnetic field, causing an overall increase in the surface

area of the electrode. The performance of the EO/EC system in TOC, COD, ammonia,

and TP removal at different constant voltages (4, 6, 8, and 10 V) was investigated, and

the results are compared in Fig. 2. With further increased voltage, the removal

efficiencies of various contaminants also increased. With increased applied voltage

from 4 V to 10 V, the TOC, ammonia, and COD removal efficiencies increased from

14.7%, 14.9%, and 17.9% to 72.5%, 97.5%, and 70.9%, respectively (Figs. 2a, 2b, and

2g). When the voltage was 4 V, the TP removal efficiency was 80.5%, and with

increased voltage from 6 V to 10 V, the TP removal efficiency was nearly 100% after 6

h of electrolysis (Fig. 2c). Increased voltage results in increased current density. For the

EO process, electron transfer on the anode occurred more quickly and produced more

intermediate products (Cl_2, HClO, and ClO^-), which accelerated the rate of direct

oxidation and indirect oxidation. For the EC process, the dissolution rate of ZVI powder

was accelerated, and the rate of compounding with phosphate in the leachate also

accelerated. Moreover, the production of $Fe(OH)_2$ and $Fe(OH)_3$ as a coagulant also

increased, accelerating the removal of organic matter and TP. As a result, 10 V was the
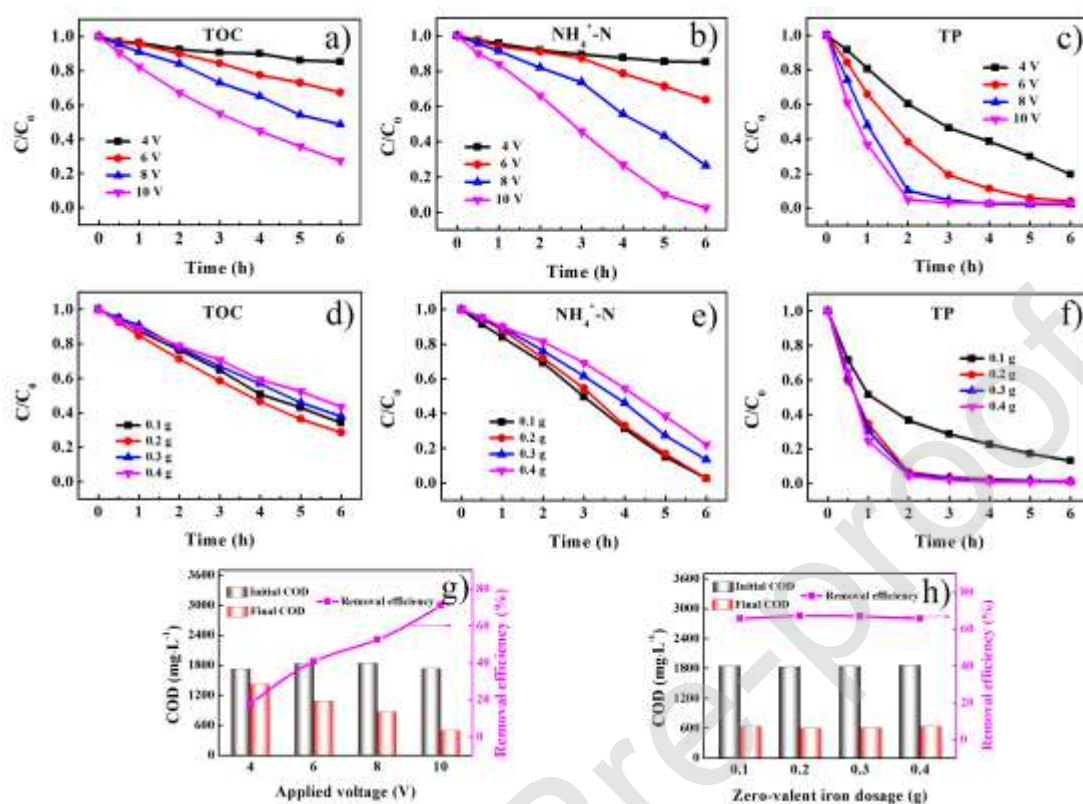
selected voltage in the next experiments.

Fig. 2. a) TOC, b) NH_4^+-N, and c) TP removal at different applied voltages; d) TOC, e) NH_4^+-N, and f) TP removal at different zero-valent iron dosages; g) COD removal at different applied voltages; and h) COD removal at different zero-valent iron dosages.

3.1.3 Zero-valent iron dosage

ZVI powder is an important part of the composite electrode, and its content may affect the EO/EC process. Too little ZVI powder might result in weak EC process, affecting the removal of TP in the leachate. By contrast, if the ZVI powder content was too high, the increase in cost and the generation of more flocs in the reaction process increased the difficulty of subsequent solid–liquid separation. Fig. 2 shows that the ZVI

dosage had little effect on the removal efficiency of organic matter (Figs. 2d and 2h).

With increased amount of ZVI powder, the TOC removal efficiency initially increased

(from 0.1 g to 0.2 g) and then decreased (from 0.2 g to 0.4 g). The maximum TOC

removal efficiency of 71.5% was obtained when the ZVI powder mass was 0.2 g; with

increased ZVI powder mass to 0.4 g, the TOC removal efficiency decreased to 55.6%.

Meanwhile, the COD removal efficiency has remained relatively stable. This finding

can be due to the fact that the amount of ZVI powder was low and the EC process was

weak. However, given that EO was dominant in the removal of TOC, the increase in

the amount of ZVI powder would suppress the EO process to some extent. Fig. 2e

shows that the greater the amount of ZVI powder used on the composite electrode, the

lower the ammonia removal efficiency. The ammonia removal efficiency decreased

from 97.5% to 77.9% when the ZVI dosage increased from 0.1 g to 0.4 g. Given that

the greater the amount of ZVI powder occupied more active sites on the RuO_2-IrO_2/Ti

plate, more electrons needed to convert ZVI into iron ions, and the rate at which Cl^- lost

electrons to form intermediates reduced under the same voltage conditions, leading to

the gradual weakening of the oxidation of the composite anode surface. However, the

small amount of ZVI powder was not conducive to TP removal. The TP removal

efficiency was 86.8% when the amount of ZVI powder in the composite electrode was

0.1 g, and when the amount of ZVI powder was higher than 0.2 g, the TP removal

efficiency can reach 99% or higher (Fig. 2f). Therefore, in combination with the

removal efficiency of various contaminants, 0.2 g was the optimal ZVI dosage in this

experiment.

3.1.4 Interelectrode gap

Experiments with different interelectrode gap sizes of 0.5, 1.0, 1.5, and 2.0 cm were conducted, and the result is illustrated in Fig. 3. TOC, ammonia, and COD removal efficiencies increased with decreased interelectrode gap. With increased interelectrode gap from 0.5 cm to 1.5 cm, the TOC, ammonia, and COD removal efficiencies decreased from 71.4%, 98.5%, and 82.9% to 56.5%, 79.8%, and 54.8%, respectively (Figs. 3a, 3b, and 3g). The continuous increase in distance between the electrodes up to 2.0 cm has little effect on contaminant removal. TOC, ammonia, and COD removal efficiencies were reduced by only 3.5%, 4.3%, and 2.0%, respectively. On one hand, increasing the distance between the electrodes caused a current intensity decrease under constant voltage conditions. On the other hand, short distance can also promote electron transfer and further enhance the organics and ammonia oxidation around the anode [32]. The difference in the TP removal in the EO/EC process was not significant at a distance from 0.5 cm to 2.0 cm (Fig. 3c). However, for short interelectrode gap, the current intensity increased and may cause short circuit [38]. Therefore, the experiment was performed with an interelectrode distance of 1 cm after balancing the removal efficiency and operational feasibility of the EO/EC process, although the short distance facilitated the removal of contaminants.
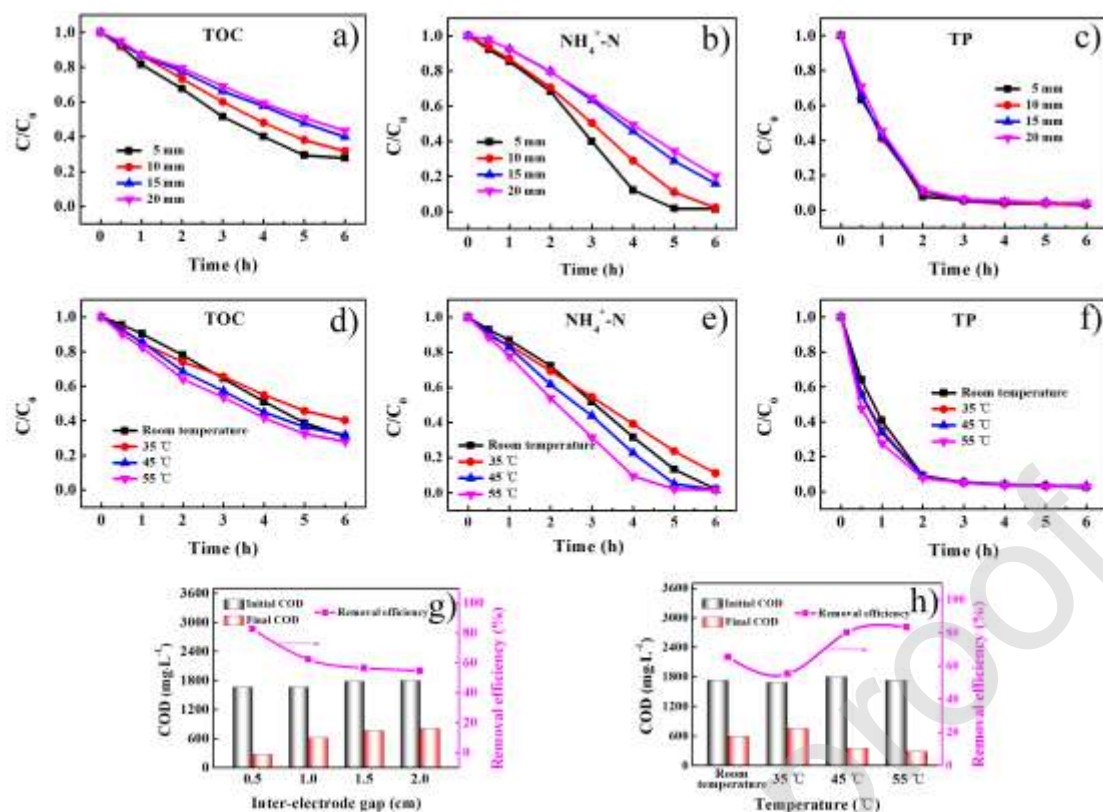
18

Fig. 3. a) TOC, b) NH_4^+-N, and c) TP removal at different interelectrode gap sizes; d) TOC, e) NH_4^+-N, and f) TP removal at different temperatures; g) COD removal at different interelectrode gaps; and h) COD removal at different temperatures.

3.1.5 Temperature

This experiment was carried out in temperature-controlled and non-temperature-controlled modes. In the temperature control mode, we set three different temperatures (35, 45, and 55 °C). The non-temperature-controlled mode was performed at room temperature (initial temperature was 23 °C). The temperature was raised from 35 °C to 55 °C to favor organic compound, ammonia, and TP removal. The TOC removal efficiency increased from 59.7% to 70.2% with increased temperature from 35 °C to 55 °C (Fig. 3d). Ammonia can almost completely be removed within 5 and 6 h when

19

the temperature was 45 and 55 °C, whereas at 35 °C, 88.8% of ammonia was removed after 6 h (Fig. 3e). This is mainly because the ionic strength and conductivity in the leachate increased as the temperature increased, thereby accelerating the rate of electron transfer. A previous study reported similar results [39], indicating that temperature is one of the important operational parameters affecting landfill leachate treatment. In the non-temperature-controlled mode, the degradation rates of TOC and ammonia were higher than that at 35 °C during the first 2.5 h of electrolysis. However, after 2.5 h, the removal efficiencies of TOC and ammonia were lower than that at 35 °C. In the non-temperature-controlled mode, as the electrolysis progressed, part of the electrical energy was converted into thermal energy, causing the change in the temperature of the leachate. The temperature change in non-temperature-controlled mode is shown in Fig. 4d. During the first 3 h of electrolysis, the temperature of the reaction system rose from the initial 23 °C to a temperature of approximately 50 °C at a relatively fast rate and gradually decreased to approximately 43 °C for the next 3 h. This finding can be due to the conversion of electrical energy into thermal energy, which caused the temperature to rise. The concentration of pollutants decreased as the EO/EC processed. The ionic strength in the leachate gradually decreased, causing the decrease in the current intensity; hence, the temperature of the reaction system tends to decrease. Without control, the temperature of the reaction system fluctuates around 45 °C after a period of time, which indicates that the removal efficiencies of contaminants were relatively close in the non-temperature-controlled mode and at the 45 °C constant temperature

mode.

3.2 Kinetics of TOC, ammonia, and TP removal

To understand the kinetics of TOC, ammonia, and TP removal, the experimental data at different temperatures were fitted with pseudo-zero, pseudo-first, or pseudo-second order kinetics, respectively (Table S1). In the removal of TOC, the pseudo-first order kinetic model fitted the experimental data better than either pseudo-zero order or pseudo-second order kinetic model; the pseudo-first order rate constant increased with increased temperature (Fig. 4a). Its removal efficiency can be expressed as:

$$\frac{d[TOC]}{dt} = -k[TOC] \tag{12}$$

After integration, the above equation gives:

$$\ln\left(\frac{[TOC]_0}{[TOC]_t}\right) = kt \tag{13}$$

where $[TOC]_0$ and $[TOC]_t$ correspond to the initial TOC concentration and the concentration, respectively, after a period of time.

Ammonia degradation was more consistent with pseudo-zero order kinetic (Table S1). Ammonia concentration decreased linearly with time at different temperatures (35, 45, and 55 °C) in the EO process (Fig. 4b). The pseudo-zero-order rate constants (k_0) were 263.11, 320.12, and 360.31 with correlation coefficients of 0.999, 0.999, and 0.994, respectively. Its removal efficiency can be expressed as:

$$\frac{d[NH_4^+\text{-}N]}{dt} = -k \tag{14}$$

After integration, the above equation gives:

$$[NH_4^+-N]_0-[NH_4^+-N]_t=kt \tag{15}$$

where $[NH_4^+-N]_0$ and $[NH_4^+-N]_t$ correspond to the initial ammonia concentration and

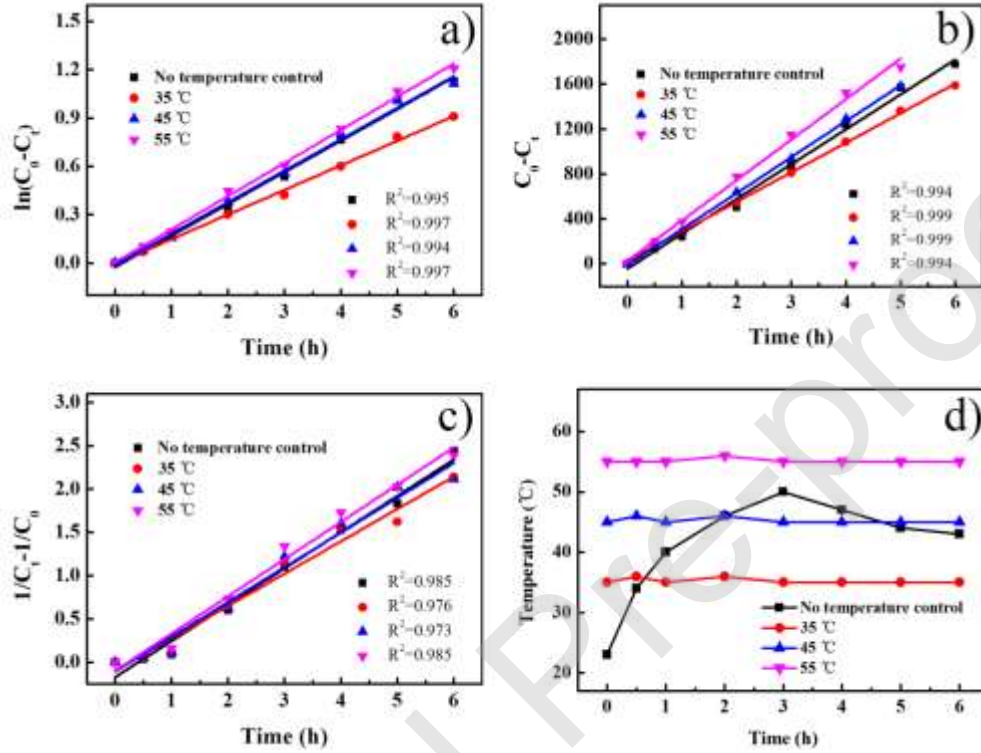the concentration after a period of time, respectively.

Fig. 4. Kinetics of a) TOC, b) NH_4^+-N, and c) TP removal; d) temperature change

during EO/EC process.

The removal of phosphorus data fitted better with the pseudo-second order kinetic

model than with either pseudo-zero or pseudo-first order kinetic models (Fig. 4c). The

pseudo-second order rate constant increased from 0.37 to 0.43 with increased

temperature from 35 °C to 55 °C. Its removal efficiency can be expressed as:

$$\frac{d[TP]}{dt}=-k[TP]^2 \tag{16}$$

After integration, the above equation gives:

$$\frac{1}{[TP]_t} - \frac{1}{[TP]_0} = kt \tag{17}$$

where $[TP]_0$ is the initial TP concentration, and $[TP]_t$ is the TP concentration after a period of time.

Furthermore, the rate constants of TOC, ammonia, and TP in the non-temperature-controlled mode were close to those at 45 °C due to the fact that the system temperature was close to 45 °C without controlling the temperature (Fig. 4d).

3.3 Characterization of precipitation

After the reaction was completed, the flocs were centrifuged and dried in a vacuum oven. The morphology and surface element composition of the precipitates were obtained by SEM-EDS, XRD, and XPS analysis. SEM image showed the mostly amorphous or ultrafine structure of the precipitates (Fig. 5a). The elemental mapping images of the precipitation with a selected area (Figs. 5b and 5c) reveal that flocs primarily contained C, O, Fe, Mg, Ca, Si, and P. This finding confirmed that some organics and phosphorus were removed by coagulation. The atomic percentage of each element on the surface of the precipitation is shown in Table S2. Ferrous ions were released into the solution and produced metal hydroxides as a coagulant to adsorb soluble or colloidal contaminants to reduce the hardness [40, 41].
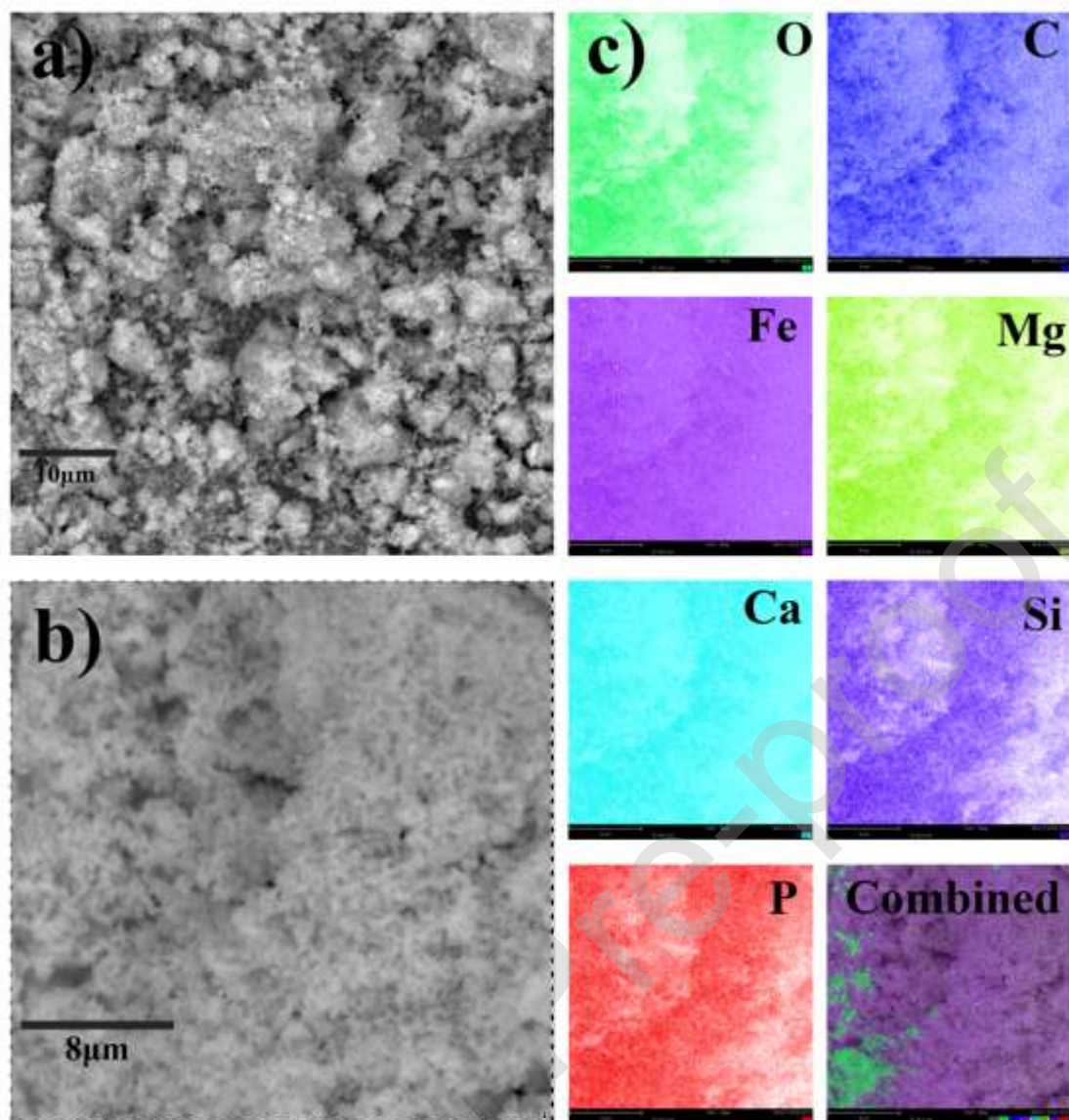
Fig. 5. SEM image and elemental mapping of the precipitates.

Fig. S2 shows the SEM image of the zero-valent iron powder before use. We can see

that the zero-valent iron powder agglomeration is obvious. The particle size of the

agglomerated iron powder was found to be below 100 μm, which confirmed that the

iron powder we used was micron-sized. The XRD patterns of the mZVI before use and

the precipitate obtained after EO/EC process are shown in Fig. 6. The apparent

reflection at 2θ=52.4° and 77.2° was found to correspond to the zero-valent iron (PDF

#87-0721). The XRD patterns from the precipitate samples showed weak peaks from

25° to 40°. These peaks are likely to indicate iron oxides and/or iron hydroxides, but

such speculation requires further analysis due to the fact that iron oxides cannot be

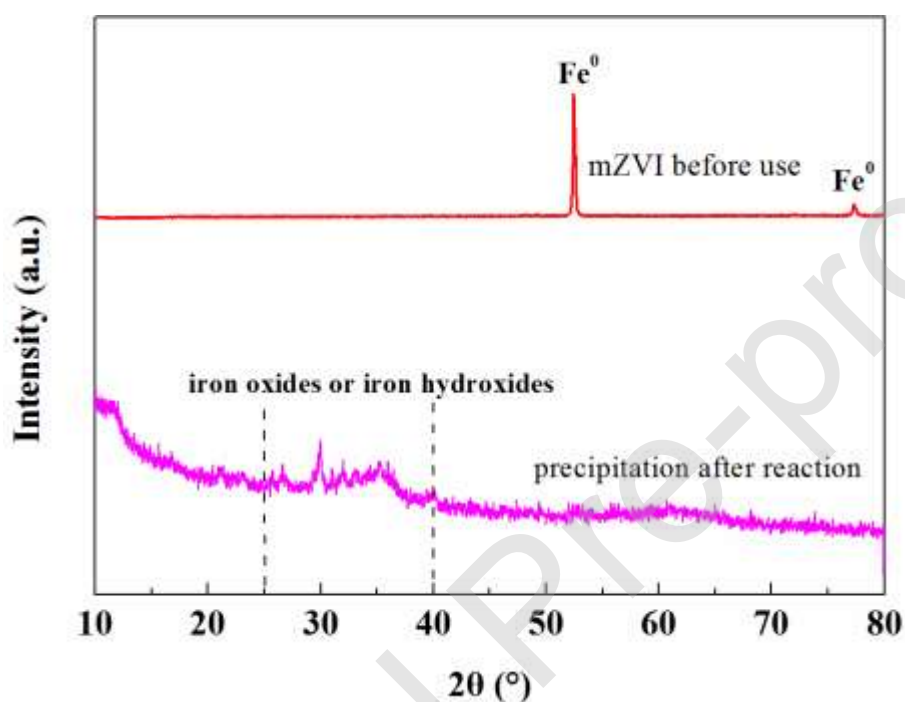easily detected by XRD due to their amorphous nature [42].

Fig. 6. XRD patterns of zero-valent iron microparticles and precipitate samples.

XPS was used to identify the chemical states of Fe, O, P, and N in the flocs produced

in the EO/EC process. The binding energy was calibrated to adventitious carbon C 1s

peak centered at 284.6 eV [43], and peak fittings were performed using XPSPeak41

software. The narrow region spectra for Fe 2p3/2 were composed of two peaks at 710.3

and 712.4 eV, respectively (Fig. 7a), indicating that ferric divalent iron and trivalent

iron existed in the precipitation after reaction [44, 45]. ZVI lost electrons to ferrous iron,

and at the same time, part of the ferrous iron is oxidized to ferric iron (Equation 9). The peak corresponding to the binding energy of Fe^0 did not appear [46], indicating that the ZVI was fully utilized and no iron powder peeled off from the RuO_2-IrO_2/Ti plate. Additionally, after peak-differentiating fitting of O 1s, three peaks were identified (Fig. 7b). The peak value of 529.7 eV corresponded to the lattice oxygen in the metal oxide (O^{2-}), the peak value of 531.1 eV was attributed to the hydroxide in the surface hydroxyls (OH^-), and the peak value of 532.1 eV was ascribed to the chemically or physically adsorbed water (H_2O_{ads}) [45, 47]. Therefore, large amounts of iron hydroxide and iron oxide were formed after the reaction. The P 2p XPS spectrum of precipitation was deconvoluted into two peaks of 132.2 and 133.2 eV, which corresponded to PO_4^{3-} and HPO_4^{2-}, respectively (Fig. 7c) [48]. This finding indicates that the surface of flocs was composed of PO_4^{3-} and HPO_4^{2-}. As noted in the case of the P 2p spectrum, the spectrum of N 1s was divided into two peaks, 399.9 and 407.2 eV (Fig. 7d), which corresponded to -NH_2 and NO_3^-, respectively [48, 49]. The presence of NO_3^- and amino groups were due to the adsorption of inorganic nitrogen and organic nitrogen in landfill leachate on the formed iron hydroxide.
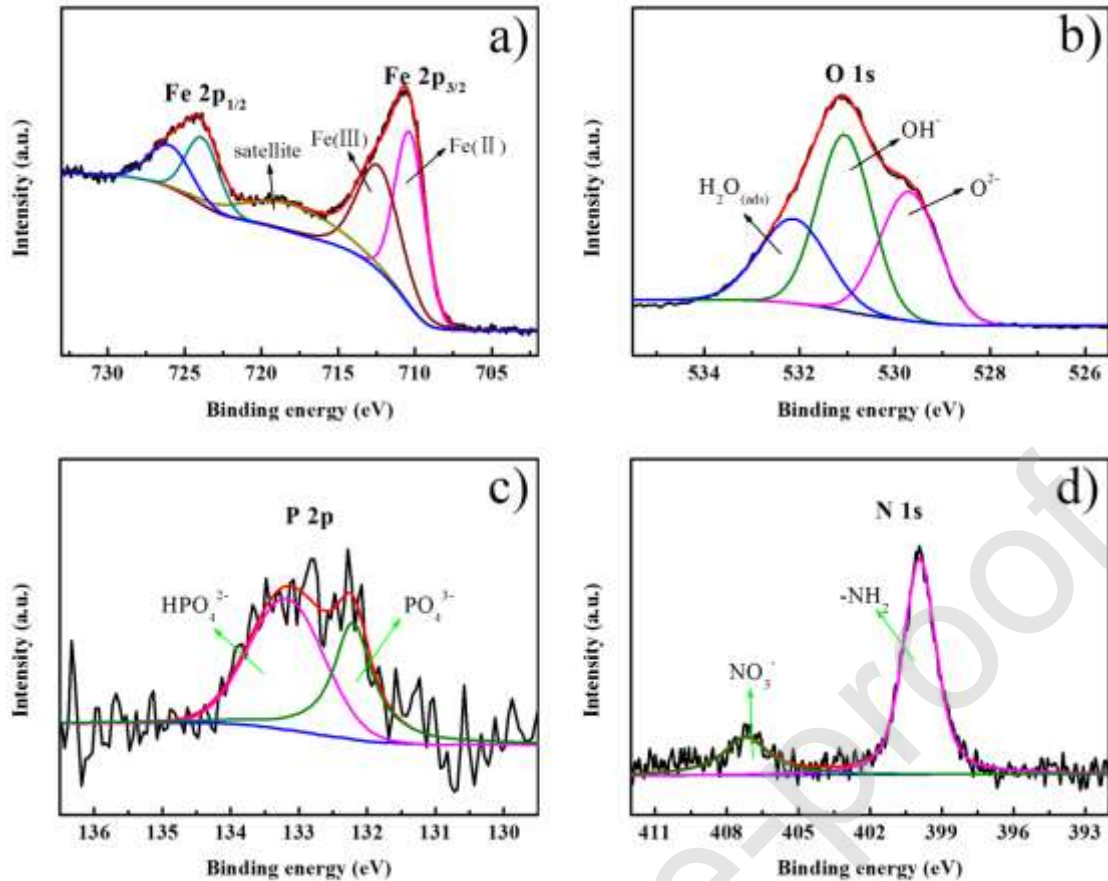
Fig. 7. XPS spectra of the surface elements of the precipitates: a) Fe, b) O, c) P, and d) N elements

4. Conclusion

The main objective of the present study was to evaluate the performance of the EO/EC reactor for the removal of TOC, ammonia, and TP from landfill leachate using mZVI-RuO$_2$-IrO$_2$/Ti. We studied the effects of important parameters, such as anode materials, applied voltage, zero-valent iron dosage, interelectrode gap, and temperature. TOC, ammonia, and TP removal efficiencies can reach 72.5%, 98.5%, and 98.6%, respectively, at the applied voltage of 10 V, ZVI dosage of 0.2 g, and interelectrode gap of 1 cm. This experiment was carried out in the temperature-controlled and non-

temperature-controlled modes. The removal efficiency of each pollutant in the non-temperature-controlled mode was similar to that when the temperature was controlled at 45 °C. TOC removal fitted the pseudo-first order kinetic model better, ammonia removal fitted the pseudo-zero order kinetic model better, and TP followed pseudo-second order kinetic model. Moreover, rate constant increased with increased temperature. SEM-EDS analysis confirmed that the hardness in the landfill leachate can be removed by EC. XPS analysis demonstrated the formation of coagulants in situ for the removal of organic compounds, TP, and heavy metals. These results show that landfill leachate can be effectively treated with mZVI-RuO_2-IrO_2/Ti anode through a combination of EO and EC processes.

Dongni Sun:
Roles/Writing - original draft; Data curation; Formal analysis; Validation; Investigation; Software; Methodology;

Xiaoting Hong:
Roles/Writing - original draft; Conceptualization; Methodology; Project administration; Funding acquisition; Writing - review & editing; Supervision; Resources; Methodology;

Zhonghua Cui: Data curation; Software;

Yingying Du: Investigation; Software;

K.S. Hui: Writing - review & editing

Enhao Zhu: Investigation;

Keming Wu: Formal analysis;

K. N. Hui: Writing - review & editing

Declaration of interests

☑ The authors declare that they have no known competing financial interests or personal relationships that could have appeared to influence the work reported in this paper.

☑The authors declare the following financial interests/personal relationships which may be considered as potential competing interests:

no

References

[1] S. Renou, J.G. Givaudan, S. Poulain, F. Dirassouyan, P. Moulin, Landfill leachate treatment: Review and opportunity, J Hazard Mater, 150 (2008) 468-493.

[2] J. Wiszniowski, D. Robert, J. Surmacz-Gorska, K. Miksch, J.V. Weber, Landfill leachate treatment methods: A review, Environ Chem Lett, 4 (2006) 51-61.

[3] K.Y. Foo, B.H. Hameed, An overview of landfill leachate treatment via activated carbon adsorption process, J Hazard Mater, 171 (2009) 54-60.

[4] C.B. Oman, C. Junestedt, Chemical characterization of landfill leachates--400 parameters and compounds, Waste Manag, 28 (2008) 1876-1891.

[5] S.H. Lin, C.C. Chang, Treatment of landfill leachate by combined electro-Fenton oxidation and sequencing batch reactor method, Wat Res, 34 (2000) 4243-4249.

[6] L.N. Wu, C.Y. Peng, S.J. Zhang, Y.Z. Peng, Nitrogen removal via nitrite from municipal landfill leachate, Journal of Environmental Sciences, 21 (2009) 1480-1485.

[7] K.J. Kennedy, E.M. Lentz, Treatment of landfill leachate using sequencing batch and continuous flow upflow anaerobic sludge blanket (UASB) reactors, Wat Res, 34 (2000) 3640-3656.

[8] T.A. Kurniawan, W.H. Lo, G.Y. Chan, Physico-chemical treatments for removal of recalcitrant contaminants from landfill leachate, J Hazard Mater, 129 (2006) 80-100.

[9] A.A. Tatsi, A.I. Zouboulis, K.A. Matis, P. Samaras, Coagulation–flocculation pretreatment of sanitary landfill leachates, Chemosphere, 53 (2003) 737-744.

[10] Y. Deng, J.D. Englehardt, Treatment of landfill leachate by the Fenton process, Water Res, 40 (2006) 3683-3694.

[11] X.Z. Li, Q.L. Zhao, X.D. Hao, Ammonium removal from landfill leachate by chemical precipitation, Waste Manag, 19 (1999) 409-415.

[12] D. Trebouet, J.P. Schlumpf, P. Jaouen, F. Quemeneur, Stabilized landfill leachate treatment by combined physicochemical–nanofiltration processes, Wat Res, 35 (2001) 2935-2942.

[13] P. Dydo, M. Turek, J. Ciba, J. Trojanowska, J. Kluczka, Boron removal from

landfill leachate by means of nanofiltration and reverse osmosis, Desalination, 185 (2005) 131-137.

[14] A. Fernandes, M.J. Pacheco, L. Ciríaco, A. Lopes, Review on the electrochemical processes for the treatment of sanitary landfill leachates: Present and future, Applied Catalysis B: Environmental, 176-177 (2015) 183-200.

[15] E. Turro, A. Giannis, R. Cossu, E. Gidarakos, D. Mantzavinos, A. Katsaounis, Electrochemical oxidation of stabilized landfill leachate on DSA electrodes, J Hazard Mater, 190 (2011) 460-465.

[16] Y. Deng, J.D. Englehardt, Electrochemical oxidation for landfill leachate treatment, Waste Manag, 27 (2007) 380-388.

[17] F.C. Moreira, R.A.R. Boaventura, E. Brillas, V.J.P. Vilar, Electrochemical advanced oxidation processes: A review on their application to synthetic and real wastewaters, Applied Catalysis B: Environmental, 202 (2017) 217-261.

[18] M. Panizza, C.A. Martinez-Huitle, Role of electrode materials for the anodic oxidation of a real landfill leachate--comparison between Ti-Ru-Sn ternary oxide, PbO_2 and boron-doped diamond anode, Chemosphere, 90 (2013) 1455-1460.

[19] A. Anglada, A. Urtiaga, I. Ortiz, D. Mantzavinos, E. Diamadopoulos, Boron-doped diamond anodic treatment of landfill leachate: evaluation of operating variables and formation of oxidation by-products, Water Res, 45 (2011) 828-838.

[20] R. Cossu, A. Polcaro, M. Lavagnolo, M. Mascia, S. Palmas, F. Renoldi, Electrochemical treatment of landfill leachate: Oxidation at Ti/PbO_2 and Ti/SnO_2 anodes, Environ Sci Technol, 32 (1998) 3570-3573.

[21] J. Wu, H. Zhang, N. Oturan, Y. Wang, L. Chen, M.A. Oturan, Application of response surface methodology to the removal of the antibiotic tetracycline by electrochemical process using carbon-felt cathode and DSA (Ti/RuO_2-IrO_2) anode, Chemosphere, 87 (2012) 614-620.

[22] P.B. Moraes, R. Bertazzoli, Electrodegradation of landfill leachate in a flow electrochemical reactor, Chemosphere, 58 (2005) 41-46.

[23] M.Y. Mollah, R. Schennach, J.R. Parga, D.L. Cocke, Electrocoagulation (EC) — science and applications, J Hazard Mater, 84 (2001) 29-41.

[24] M.Y. Mollah, P. Morkovsky, J.A. Gomes, M. Kesmez, J. Parga, D.L. Cocke, Fundamentals, present and future perspectives of electrocoagulation, J Hazard Mater, 114 (2004) 199-210.

[25] G.H. Chen, Electrochemical technologies in wastewater treatment, Separation and Purification Technology, 38 (2004) 11-41.

[26] S. Top, E. Sekman, S. Hoşver, M.S. Bilgili, Characterization and electrocaogulative treatment of nanofiltration concentrate of a full-scale landfill leachate treatment plant, Desalination, 268 (2011) 158-162.

[27] F. Bouhezila, M. Hariti, H. Lounici, N. Mameri, Treatment of the OUED SMAR town landfill leachate by an electrochemical reactor, Desalination, 280 (2011) 347-353.

[28] F. Ilhan, U. Kurt, O. Apaydin, M.T. Gonullu, Treatment of leachate by electrocoagulation using aluminum and iron electrodes, J Hazard Mater, 154 (2008) 381-389.

[29] A.H. Mahvi, S.J. Ebrahimi, A. Mesdaghinia, H. Gharibi, M.H. Sowlat, Performance evaluation of a continuous bipolar electrocoagulation/electrooxidation-electroflotation (ECEO-EF) reactor designed for simultaneous removal of ammonia and phosphate from wastewater effluent, J Hazard Mater, 192 (2011) 1267-1274.

[30] Y. Esfandyari, Y. Mahdavi, M. Seyedsalehi, M. Hoseini, G.H. Safari, M.G. Ghozikali, H. Kamani, J. Jaafari, Degradation and biodegradability improvement of the olive mill wastewater by peroxi-electrocoagulation/electrooxidation-electroflotation process with bipolar aluminum electrodes, Environ Sci Pollut Res Int, 22 (2015) 6288-6297.

[31] J. Li, Z.H. Yang, H.Y. Xu, P.P. Song, J. Huang, R. Xu, Y.J. Zhang, Y. Zhou, Electrochemical treatment of mature landfill leachate using $Ti/RuO_2–IrO_2$ and Al electrode: optimization and mechanism, RSC Advances, 6 (2016) 47509-47519.

[32] J. Ding, L. Wei, H. Huang, Q. Zhao, W. Hou, F.T. Kabutey, Y. Yuan, D.D.

Dionysiou, Tertiary treatment of landfill leachate by an integrated Electro-Oxidation/Electro-Coagulation/Electro-Reduction process: Performance and mechanism, J Hazard Mater, 351 (2018) 90-97.

[33] Y. Gendel, O. Lahav, Revealing the mechanism of indirect ammonia electrooxidation, Electrochimica Acta, 63 (2012) 209-219.

[34] N. Fan, Z. Li, L. Zhao, N. Wu, T. Zhou, Electrochemical denitrification and kinetics study using $Ti/IrO_2–TiO_2–RuO_2$ as the anode and Cu/Zn as the cathode, Chemical Engineering Journal, 214 (2013) 83-90.

[35] Y. Tian, W. He, D. Liang, W. Yang, B.E. Logan, N. Ren, Effective phosphate removal for advanced water treatment using low energy, migration electric-field assisted electrocoagulation, Water Res, 138 (2018) 129-136.

[36] F. Akbal, S. Camcı, Comparison of Electrocoagulation and Chemical Coagulation for Heavy Metal Removal, Chemical Engineering & Technology, 33 (2010) 1655-1664.

[37] L. Xu, X. Xu, G. Cao, S. Liu, Z. Duan, S. Song, M. Song, M. Zhang, Optimization and assessment of Fe-electrocoagulation for the removal of potentially toxic metals from real smelting wastewater, J Environ Manage, 218 (2018) 129-138.

[38] N. Mameri, H. Lounici, D. Belhocine, H. Grib, B. Bariou, A.R. Yeddou, Defluoridation of septentrional sahara water of north africa by electrocoagulation process using bipolar aluminium electrodes, Wat Res, 32 (1998) 1604-1612.

[39] M. Panizza, M. Delucchi, I. Sirés, Electrochemical process for the treatment of landfill leachate, J Appl Electrochem, 40 (2010) 1721-1727.

[40] M. Malakootian, H.J. Mansoorian, M. Moosazadeh, Performance evaluation of electrocoagulation process using iron-rod electrodes for removing hardness from drinking water, Desalination, 255 (2010) 67-71.

[41] S. Zhao, G. Huang, G. Cheng, Y. Wang, H. Fu, Hardness, COD and turbidity removals from produced water by electrocoagulation pretreatment prior to Reverse Osmosis membranes, Desalination, 344 (2014) 454-462.

[42] I.H. Yoon, G. Yoo, H.J. Hong, J. Kim, M.G. Kim, W.K. Choi, J.W. Yang, Kinetic

study for phenol degradation by ZVI-assisted Fenton reaction and related iron corrosion investigated by X-ray absorption spectroscopy, Chemosphere, 145 (2016) 409-415.

[43] X. Hong, E. Zhu, Z. Ye, K.S. Hui, K.N. Hui, Enhanced phosphate removal under an electric field via multiple mechanisms on MgAl-LDHs/AC composite electrode, Journal of Electroanalytical Chemistry, 836 (2019) 16-23.

[44] S. Bae, W. Lee, Influence of riboflavin on nanoscale zero-valent iron reactivity during the degradation of carbon tetrachloride, Environ Sci Technol, 48 (2014) 2368-2376.

[45] W.M. Chen, A.P. Zhang, Z.P. Gu, Q.B. Li, Enhanced degradation of refractory organics in concentrated landfill leachate by Fe^0/H_2O_2 coupled with microwave irradiation, Chemical Engineering Journal, 354 (2018) 680-691.

[46] S. Bae, W. Lee, Inhibition of nZVI reactivity by magnetite during the reductive degradation of 1,1,1-TCA in nZVI/magnetite suspension, Applied Catalysis B: Environmental, 96 (2010) 10-17.

[47] C. Tan, Y. Dong, D. Fu, N. Gao, J. Ma, X. Liu, Chloramphenicol removal by zero valent iron activated peroxymonosulfate system: Kinetics and mechanism of radical generation, Chemical Engineering Journal, 334 (2018) 1006-1015.

[48] H. Yin, M. Kong, Simultaneous removal of ammonium and phosphate from eutrophic waters using natural calcium-rich attapulgite-based versatile adsorbent, Desalination, 351 (2014) 128-137.

[49] O. Rosseler, M. Sleiman, V.N. Montesinos, A. Shavorskiy, V. Keller, N. Keller, M.I. Litter, H. Bluhm, M. Salmeron, H. Destaillats, Chemistry of NO_x on TiO_2 Surfaces Studied by Ambient Pressure XPS: Products, Effect of UV Irradiation, Water, and Coadsorbed K(.), J Phys Chem Lett, 4 (2013) 536-541.